RESEARCH ARTICLE

Nodule Parenchyma–Specific Expression of the *Sesbania rostrata* Early Nodulin Gene *SrEnod2* Is Mediated by Its 3′ Untranslated Region

Rujin Chen,[a,b,1] David L. Silver,[a,c,2] and Frans J. de Bruijn[a,c,d,3]

[a] Michigan State University Department of Energy Plant Research Laboratory, East Lansing, Michigan 48824-1312
[b] Department of Biochemistry, Michigan State University, East Lansing, Michigan, 48824-1312
[c] Genetics Program, Michigan State University, East Lansing, Michigan 48824-1312
[d] Department of Microbiology, Michigan State University, East Lansing, Michigan 48824-1312

The early nodulin *Enod2* gene encodes a putative hydroxyproline-rich cell wall protein and is expressed exclusively in the nodule parenchyma cell layer. The latter finding suggests that the Enod2 protein may contribute to the special morphological features of the nodule parenchyma and to the creation of an oxygen diffusion barrier. The *Enod2* gene of the stem-nodulating legume *Sesbania rostrata* (*SrEnod2*) is induced specifically in roots by the plant hormone cytokinin, and this induction occurs at a post-transcriptional level. Here, we characterize the *cis* determinant(s) in the *SrEnod2* locus responsible for nodule parenchyma–specific expression and show that the 3′ untranslated region (UTR) of the *SrEnod2* gene is both required and sufficient for directing chimeric reporter gene expression in the nodule parenchyma of transgenic *Lotus corniculatus* plants. Moreover, we show that the *SrEnod2* 3′ UTR does not act as a tissue-specific enhancer element. By conducting a detailed deletion analysis of the 5′ and 3′ *SrEnod2* regions, we delimited the minimal promoter of the *SrEnod2* gene, and it appears that the 5′ flanking sequences are not essential for nodule parenchyma–specific expression. This finding is in contrast with the report that the 5′ upstream region of the soybean *Enod2* gene directs nodule parenchyma–specific expression, indicating that different mechanisms may be involved in regulating the expression of these two genes. We definitively demonstrate that the *cis* element(s) for tissue-specific expression is located within the 3′ UTR of a plant nuclear gene.

INTRODUCTION

Symbiotic interactions between legume plants and soil bacteria of the genera *Rhizobium*, *Bradyrhizobium*, and *Azorhizobium* result in the formation of new plant organs, namely, root and stem nodules. Nodule formation is initiated by the exchange and recognition of signal molecules between the symbiotic partners (Long, 1989; Fisher and Long, 1992). Flavonoids and isoflavonoids secreted by roots of legume plants serve as chemoattractants as well as inducers of the bacterial nodulation (*nod*) genes. Expression of the *nod* genes, in turn, results in both the synthesis of lipochitooligosaccharides, known as Nod factors, which are capable of initiating the process of nodule formation (Lerouge et al., 1990; Truchet et al., 1991; Vijn et al., 1993; Yang et al., 1994), and the signal transduction pathway responsible for activating nodulin gene expression (Pingret et al., 1998). When infected with rhizobia, roots of legume plants undergo specific morphological changes, such as root hair deformation and curling, cortical cell division, formation of infection threads, and the release of bacteria via endocytosis, leading ultimately to the development of mature nodules (reviewed in Verma and Delauney, 1988; Gloudemans and Bisseling, 1989; Nap and Bisseling, 1990; Kijne, 1992; Mylona et al., 1995).

Concomitant with the observed morphological changes in the infected plant roots, the expression of specific plant genes is induced or enhanced. These genes are referred to as early- or late-nodulin genes (van Kammen, 1984). Early-nodulin genes are activated at early stages of nodule development, well before the onset of nitrogen fixation. Their gene products are involved in the infection process and nodule ontogeny. Late-nodulin genes are first expressed

around the onset of nitrogen fixation. Their products are generally responsible for nodule functioning (Nap and Bisseling, 1990; de Bruijn and Schell, 1992).

The *Enod2* gene is an early-nodulin gene that was first identified by differential screening of a soybean root nodule cDNA library (Franssen et al., 1987). Isolation of *Enod2* homologs from other legumes and subsequent DNA sequence comparisons have shown that the *Enod2* gene is highly conserved among leguminous plants (Franssen et al., 1987; Dickstein et al., 1988; Govers et al., 1990; Szczyglowski and Legocki, 1990; Van de Wiel et al., 1990a; Dehio and de Bruijn, 1992). The amino acid sequence derived from the soybean *Enod2* cDNA clone revealed that the Enod2 protein is very proline rich and is composed mainly of two repeating pentapeptides, Pro-Pro-His-Glu-Lys and Pro-Pro-Glu-Tyr-Gln (Franssen et al., 1987; Van de Wiel et al., 1990a). The Enod2 proteins of other legumes appear to be composed of the same or similar repeating pentapeptides (Dickstein et al., 1988; Szczyglowski and Legocki, 1990; Van de Wiel et al., 1990a; Dehio and de Bruijn, 1992). A putative signal peptide is present at the N terminus of all of the Enod2 proteins identified thus far, and the amino acid sequences of both pea and soybean Enod2 proteins highly resemble a hydroxy-proline-rich cell wall protein identified in soybean seed cell walls (Averyhart-Fullard et al., 1988; Van de Wiel et al., 1990a). Therefore, it has been proposed that the Enod2 protein is a cell wall protein (Van de Wiel et al., 1990a).

The *Enod2* gene is expressed during early stages of nodule organogenesis (Franssen et al., 1987; Van de Wiel et al., 1990a; Dehio and de Bruijn, 1992). It has been shown that this early-nodulin gene is expressed also in empty nodules induced by certain *Rhizobium* strains on the roots of soybean and alfalfa (Finan et al., 1985; Franssen et al., 1987; Dickstein et al., 1988). These empty nodules contain neither infection threads nor intracellular bacteroids. Expression of the *Enod2* gene also has been demonstrated in "pseudo-nodules" induced by auxin transport inhibitors (Hirsch et al., 1989; Van de Wiel et al., 1990b) or by *Rhizobium* nodulation-deficient (Nod⁻) mutants secreting the cytokinin *trans*-zeatin (Cooper and Long, 1994). The expression of the *Enod2* gene in these empty/pseudonodules strongly suggests that the Enod2 protein is not involved in the infection process per se but may play a role in nodule ontogeny.

The finding that the *Enod2* gene is expressed in alfalfa pseudonodules induced by auxin transport inhibitors (Hirsch et al., 1989) extends the observations made several decades ago suggesting that plant hormones are involved in the induction of nodules on plant roots (Thimann, 1936; Arora et al., 1959; Libbenga et al., 1973; reviewed in Hirsch, 1992; Verma, 1992). In fact, plant hormones clearly appear to be involved in the expression of the *Enod2* gene; Dehio and de Bruijn (1992) first demonstrated that the expression of the *Enod2* gene of *Sesbania rostrata* is specifically upregulated in roots after the application of cytokinin. Similar results have been reported for the alfalfa *Enod2* gene (Hirsch et al., 1993), although the size of the cytokinin-enhanced

Enod2 transcript in roots is larger than that observed in alfalfa nodules.

In situ hybridization studies have demonstrated that the soybean *Enod2* gene is expressed in the nodule parenchyma and in the nodule tissue surrounding the vascular bundle that connects the nodule to the root central cylinder (Van de Wiel et al., 1990a). Low levels of the *Enod2* transcript also have been found in the nodule endodermis and the nodule outer cortical cells directly adjacent to the endodermis (Van de Wiel et al., 1990a). The nodule parenchyma is composed of several layers of cells, with fewer and smaller intercellular spaces than most other cortical cells (Van de Wiel et al., 1990a). The compact structure of these cell layers has suggested to various investigators that they may be involved in forming an oxygen diffusion barrier (Tjepkema and Yocum, 1974; Witty et al., 1986; Nap and Bisseling, 1990; Van de Wiel et al., 1990a). Because the Enod2 protein is localized in the same cell layers, it has been hypothesized to contribute to the special morphology of the nodule parenchyma and therefore to the formation of the oxygen barrier (Nap and Bisseling, 1990; Van de Wiel et al., 1990a). However, no experimental evidence supporting this hypothesis exists.

Recently, considerable efforts have been made to understand how *Enod2* gene expression is controlled in developing soybean and *S. rostrata* nodules and in roots of *S. rostrata* plants after cytokinin treatment (Lauridsen et al., 1993; de Bruijn et al., 1994; Silver et al., 1996). We have shown that the cytokinin-mediated upregulation of the *SrEnod2* gene in uninfected roots of *S. rostrata* occurs post-transcriptionally and mainly in the cytoplasm, requires protein synthesis, and appears to involve protein phosphorylation (Silver et al., 1996). We also have reported that a 3-kb 5′ upstream region of the *SrEnod2* gene failed to consistently direct the expression of the *uidA* reporter gene (*gus*; Jefferson et al., 1987) in the nodule parenchyma of transgenic *Lotus corniculatus* plants (de Bruijn et al., 1994). In contrast, a 3-kb 5′ region of the soybean *Enod2(B)* gene has been shown to direct reporter gene expression in the nodule parenchyma of transgenic *L. corniculatus* plants (Lauridsen et al., 1993). Here, we provide a detailed analysis of DNA sequence determinants in the *SrEnod2* locus responsible for tissue-specific expression in nodules. We conclude from this analysis that although the 5′ proximal region of the *SrEnod2* gene is required for gene expression, the 3′ untranslated region (3′ UTR) of the *SrEnod2* gene contains DNA sequence determinants responsible and sufficient for nodule parenchyma–specific induction.

RESULTS

Localization of the *SrEnod2* Transcript in the Parenchyma of *S. rostrata* Stem and Root Nodules

The tropical legume *S. rostrata* forms nodules on both roots and stems after infection with *A. caulinodans* ORS571 (Dreyfus

and Dommergues, 1981; de Bruijn, 1989). Because the primitive crack entry–mediated infection process of both stems and roots makes the symbiotic interaction between *S. rostrata* and *A. caulinodans* ORS571 unique (Tsien et al., 1983; de Bruijn, 1989; Ndoye et al., 1994), we studied the tissue-specific expression of the *SrEnod2* gene in *S. rostrata* stem and root nodules. The results presented in Figure 1 show that the *SrEnod2* gene is expressed in the nodule parenchyma cells of both stem and root nodules (Figures 1A and 1B). In both types of nodules, hybridization signals were also observed in cells immediately adjacent to the nodule vascular tissue (Figures 1C and 1D).

Moreover, in stem nodules, hybridization signals also were detected in cell layers corresponding to the nodule endodermis (Figure 1D, arrowhead). Expression of the *SrEnod2* gene was not observed in other nodule cells. Therefore, the expression pattern of the *SrEnod2* gene in the parenchyma cells of *S. rostrata* stem and root nodules appears to be similar to that of the *Enod2* genes of other legumes (Van de Wiel et al., 1990a).

The 3′ Flanking Region of the *SrEnod2* Gene Is Required for Gene Expression in the Nodule Parenchyma

To identify DNA sequence determinants responsible for nodule parenchyma–specific expression of the *SrEnod2* gene, we constructed a chimeric reporter gene fusion (*gus*; Jefferson, 1987; Jefferson et al., 1987) in which the 5′ and 3′ flanking regions of the *SrEnod2* gene were connected to the coding region of the *gus* reporter gene (5′ *SrEnod2*–*gus*–3′ *SrEnod2*; Figure 2A, construct 1). A construct containing the 3′ terminator region of the nopaline synthase gene (3′ *nos*) was used as a control (5′ *SrEnod2*–*gus*–3′ *nos*; Figure 2A, construct 2). These two constructs were introduced into *L. corniculatus* plants by *Agrobacterium rhizogenes*–mediated plant transformation (Szabados et al., 1990), and their presence in transgenic plants was verified by DNA gel blotting (data not shown). Expression of the *gus* reporter gene was determined histochemically and quantitatively in tissues of transgenic plants 21 days after inoculation with rhizobia.

Histochemical staining revealed that *gus* reporter gene expression was visible as a ringlike pattern in cross-sections of mature nodules expressing the 5′ *SrEnod2*–*gus*–3′ *SrEnod2* construct (Figure 3B). No *gus* reporter gene expression could be detected in leaves, stems, or uninfected roots of the transgenic plants (Figure 2A). However, weak reporter gene expression could be detected in regions near the root tips of some transgenic plants, but only after infection with rhizobia (Figure 3B). When the 3′ *nos* region was present instead of the *SrEnod2* 3′ region, no reporter gene expression could be detected in any tissues of the transgenic plants (Figures 2A and 3A).

Dark-field microscopy revealed that the expression of the 5′ *SrEnod2*–*gus*–3′ *SrEnod2* construct was localized in the nodule parenchyma and vascular tissues (Figure 3D). A low

level of GUS activity was detected also in the outer cortex of the nodule. The histochemical staining pattern of the reporter gene constructs correlates well with the in situ *Enod2* mRNA hybridization pattern found in *S. rostrata* nodules (Figure 1) and those observed for other legumes (Van de Wiel et al., 1990a). The only exception to this correlation is that our reporter gene construct also was expressed in the
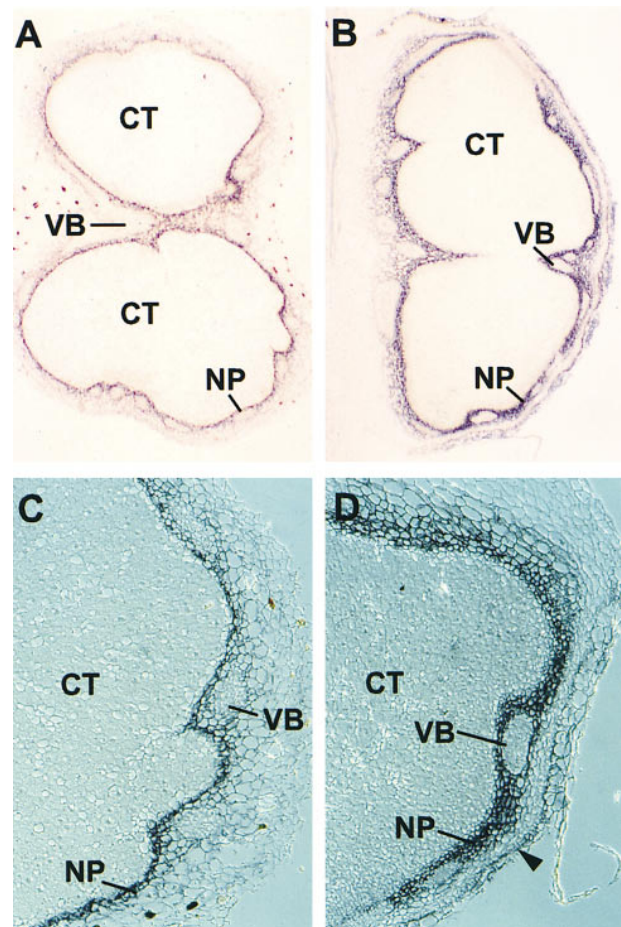
Figure 1. In Situ Localization of *SrEnod2* Gene Expression.

Sections (7 μm) of *S. rostrata* root and stem nodules harvested 6 days after inoculation with *A. caulinodans* ORS571 were hybridized with a digoxigenin-labeled antisense RNA probe derived from the *SrEnod2* coding region. Pink and black colors indicate hybridization signals. No signals were observed in neighboring sections hybridized with the sense probe (data not shown).
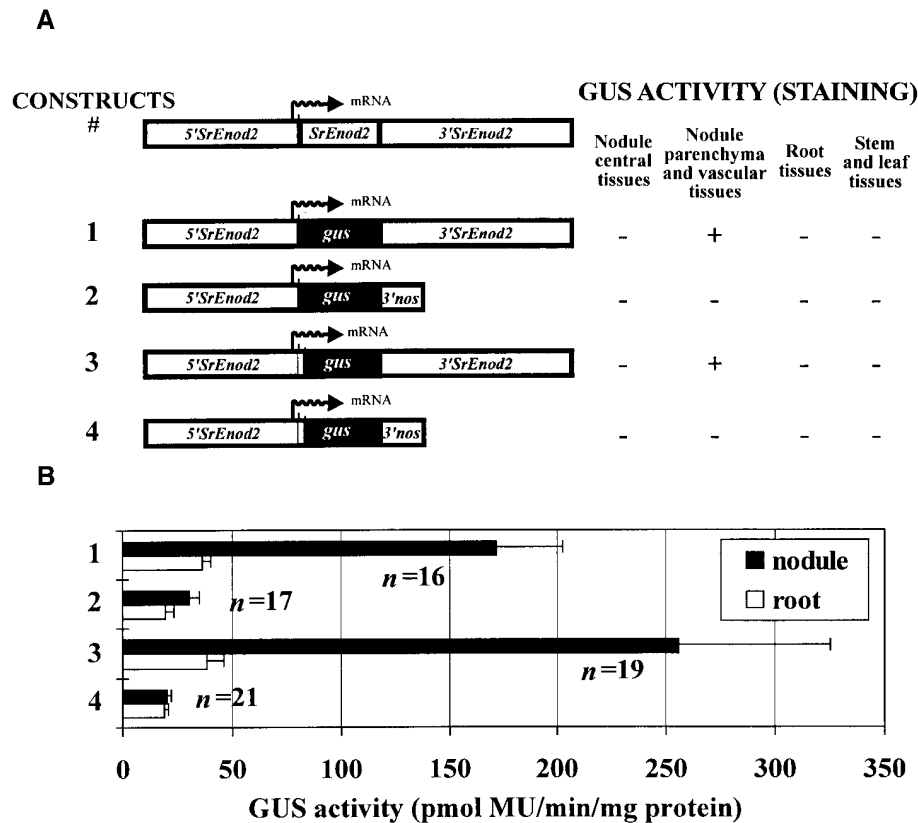
(A) Section of a root nodule.
(B) Section of a stem nodule.
(C) Magnification of the section shown in **(A)**.
(D) Magnification of the section shown in **(B)**. The arrowhead indicates expression in the nodule endodermis.
CT, central tissue; NP, nodule parenchyma; VB, vascular bundle.

A

B

Figure 2. Structure of *gus* Fusion Constructs and Determination of GUS Activity in Transgenic *L. corniculatus* Plants.

(A) Structure of *gus* fusion constructs. The construct numbers are listed at left. The boxes in black and white represent *gus*, *SrEnod2*, and *nos* gene sequences, as indicated. The vertical lines and wavy arrows represent the transcriptional start site of the *SrEnod2* gene, as determined by Dehio and de Bruijn (1992). The short vertical bars attached to the boxes immediately downstream of the transcriptional start sites represent the translational start of the corresponding genes. The thin open boxes immediately downstream of the *SrEnod2* translational start site represent a 75-bp putative signal peptide sequence. (+) and (−) designate positive and negative staining results, respectively.
(B) Quantification of GUS activity in transgenic *L. corniculatus* plants. The data shown represent mean values in units of picomoles of 4-methyl-umbelliferone (MU) per minute per milligram of protein. The error bars represent the standard deviation of the mean. *n* indicates the number of transgenic plants tested. Construct numbers are listed at left.

nodule vascular tissue. Dark-field microscopy confirmed that no GUS activity was detectable in nodules of transgenic plants harboring the 5′ *SrEnod2–gus*–3′ *nos* construct (Figure 3C).
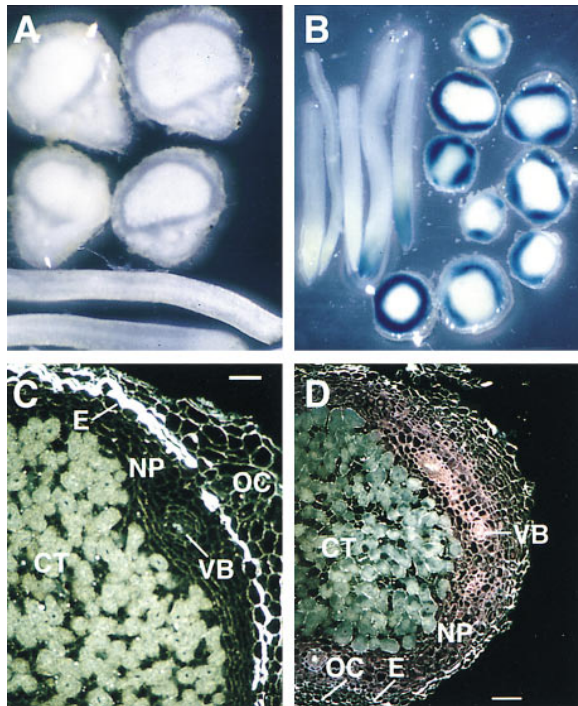
The histochemical staining analysis revealed limited variations in the expression of the reporter gene. Twelve of 17 transgenic plants harboring 5′ *SrEnod2–gus*–3′ *SrEnod2* (Figure 2A, construct 1) had significant reporter gene expression in nodules, five plants were inactive, and one plant had a high level of reporter gene expression in both nodules and infected roots (data not shown). A variation in reporter gene expression pattern was observed also in one of 18 transgenic plants harboring the 5′ *SrEnod2–gus*–3′ *nos* construct, which had a low level of *gus* expression in the nodule vascular tissue (data not shown). It is likely that these variations are due to "position effects" (Odell et al., 1985; Sanders

et al., 1987; Benfey et al., 1989); therefore, these transgenic plants were excluded from further analysis.

GUS activity in nodules and infected roots of transgenic plants was quantified using a fluorometric assay. As shown in Figure 2B, GUS activity was detected only in nodules of transgenic plants harboring the 5′ *SrEnod2–gus*–3′ *SrEnod2* construct. No GUS activity was detected in nodules of transgenic plants harboring the 5′ *SrEnod2–gus*–3′ *nos* construct, confirming the results of the histochemical staining analysis. These results strongly suggest that the 3′ region of the *SrEnod2* gene is required for tissue-specific reporter gene expression in transgenic plants.

In previous studies examining the interaction of DNA binding proteins (*trans*-acting factors) with the *SrEnod2* locus, a specific protein–DNA interaction with sequences encoding

the putative *SrEnod2* leader peptide was identified (A. Goel and F.J. de Bruijn, unpublished data). Therefore, we also examined the role of the *SrEnod2* putative signal peptide sequence in modulating *gus* reporter gene expression. A 75-bp nucleotide sequence encoding the N-terminal putative signal peptide of 25 amino acids (Dehio and de Bruijn, 1992) was transcriptionally fused to the truncated *SrEnod2* 5′ flanking region previously used (Figure 2A, constructs 1 and 2). The transcriptional fusions (Figure 2A, constructs 3 and 4) displayed a pattern and level of reporter gene expression similar to the original truncated constructs lacking the leader se-
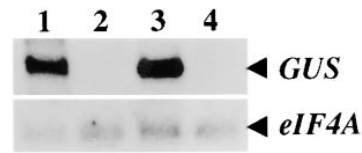

Figure 4. RNA Gel Blot Analysis of *gus* Reporter Gene Expression in Transgenic Nodules Harboring the Reporter Gene Constructs 1 to 4 (Shown in Figure 2A).

The lane numbers correspond to the construct numbers in Figure 2A. Two micrograms of poly(A)$^+$ RNA was loaded in each lane and hybridized with a ^{32}P-labeled riboprobe derived from the *gus* coding region. The same blot was stripped and rehybridized with a ^{32}P-labeled *eIF4A* probe (Taylor et al., 1993) as a loading control.

quence (Figure 2B). Therefore, the putative signal peptide sequence does not appear to influence the expression of the reporter gene when fused to it in a transcriptional configuration.

gus Reporter Gene Activities Correlate with Steady State *gus* mRNA Levels in Transgenic Nodules

RNA gel blot analysis was performed to determine whether the *gus* reporter gene activities observed correlate with the levels of the *gus* transcript accumulation. As shown in Figure 4, nodule poly(A)$^+$ RNA isolated from a pool of three independent transgenic plants harboring constructs containing the *SrEnod2* 3′ region strongly hybridized with the riboprobe prepared from the *gus* coding region (Figure 4, lanes 1 and 3). The transcript detected was ∼2.3 kb in length, as expected. In contrast, nodule poly(A)$^+$ RNA isolated from a pool of three independent transgenic plants harboring constructs containing the 3′ *nos* terminator did not hybridize with the *gus* probe (Figure 4, lanes 2 and 4). The same blot was stripped and reprobed with an *eIF4A* gene probe (Taylor et al., 1993) to standardize loading. The signal peptide sequence of the *SrEnod2* gene was not found to influence the accumulation of the reporter gene transcript when fused in a transcriptional configuration to the *gus* coding region (Figure 4, lanes 1 and 3).

These data clearly show that the accumulation of the reporter gene transcript correlates well with the *gus* reporter activity detected in transgenic plants. In addition, they reveal that the reporter gene transcript accumulates in transgenic plants harboring the constructs containing the *SrEnod2* 3′ region but not the 3′ *nos* terminator.

The 3′ Region of the *SrEnod2* Gene Contains Sequence Determinants Sufficient for Expression in the Nodule Parenchyma

To examine further the role of the *SrEnod2* 3′ region in directing nodule parenchyma–specific expression, we constructed

Figure 3. Microscopic Analysis of the Expression of Reporter Gene Constructs in Transgenic *L. corniculatus* Plants.

(A) Hand-cut sections of transgenic nodules harboring the 5′ *SrEnod2–gus–*3′ *nos* construct (Figure 2A, construct 2). The grayish blue hue of the nodule parenchyma area in these sections does not indicate GUS activity but is an artifact of the microscopy conditions used (reflection of light).

(B) Hand-cut sections of transgenic nodules harboring the 5′ *SrEnod2–gus–*3′ *SrEnod2* construct (Figure 2A, construct 1). GUS activity (blue color) can be seen in the nodule parenchyma and in regions near the root tip of some infected roots.

(C) Dark-field microscopy of a 10-μm section of one of the transgenic nodules shown in **(A)**.

(D) Dark-field microscopy of a 10-μm section of one of the transgenic nodules shown in **(B)**. GUS activity (brick-red color) can be seen in the nodule parenchyma, vascular, and outer cortical tissues. CT, central tissue; E, endodermis; NP, nodule parenchyma; OC, outer cortical tissue; VB, vascular bundle. Bars in **(C)** and **(D)** = 100 μm.

additional chimeric reporter gene fusions containing heterologous promoters, for example, the leghemoglobin (*Srglb3*) promoter from *S. rostrata* (Szabados et al., 1990; Szczyglowski et al., 1994), the *nos* minimal promoter (−150 to +1 bp; Depicker et al., 1982; Ebert et al., 1987), and the cauliflower mosaic virus (CaMV) 35S minimal promoter (−90 to +6 bp, domain A; Franck et al., 1980; Pietrzak et al., 1986; Benfey et al., 1989). The resulting constructs (see Figure 5A) were introduced into *L. corniculatus*, and the expression of the *gus* gene was determined histochemically and quantitatively.

It was shown previously that a 5′ *Srglb3–gus*–3′ *nos* construct (Figure 5A, construct 5) is expressed exclusively in the infected cells of transgenic nodules (Szabados et al., 1990; Szczyglowski et al., 1994; see also Figures 6A and 6C). However, when the 3′ *nos* terminator was replaced by the *SrEnod2* 3′ region (Figure 5A, construct 6), GUS activity was detected not only in the infected cells of transgenic nodules but also in the nodule parenchyma cells, the vascular tissue, and the outer cortex (Figures 6B and 6D). Dark-field microscopy revealed that GUS expression directed by the 5′ *Srglb3–gus*–3′ *SrEnod2* construct also could be detected in the central uninfected (interstitial) cells of transgenic nodules (Figure 6D) but could not be detected in transgenic stem, leaf, and root tissues (data summarized in Figure 5A). This expression pattern suggests an additive effect of the leghemoglobin
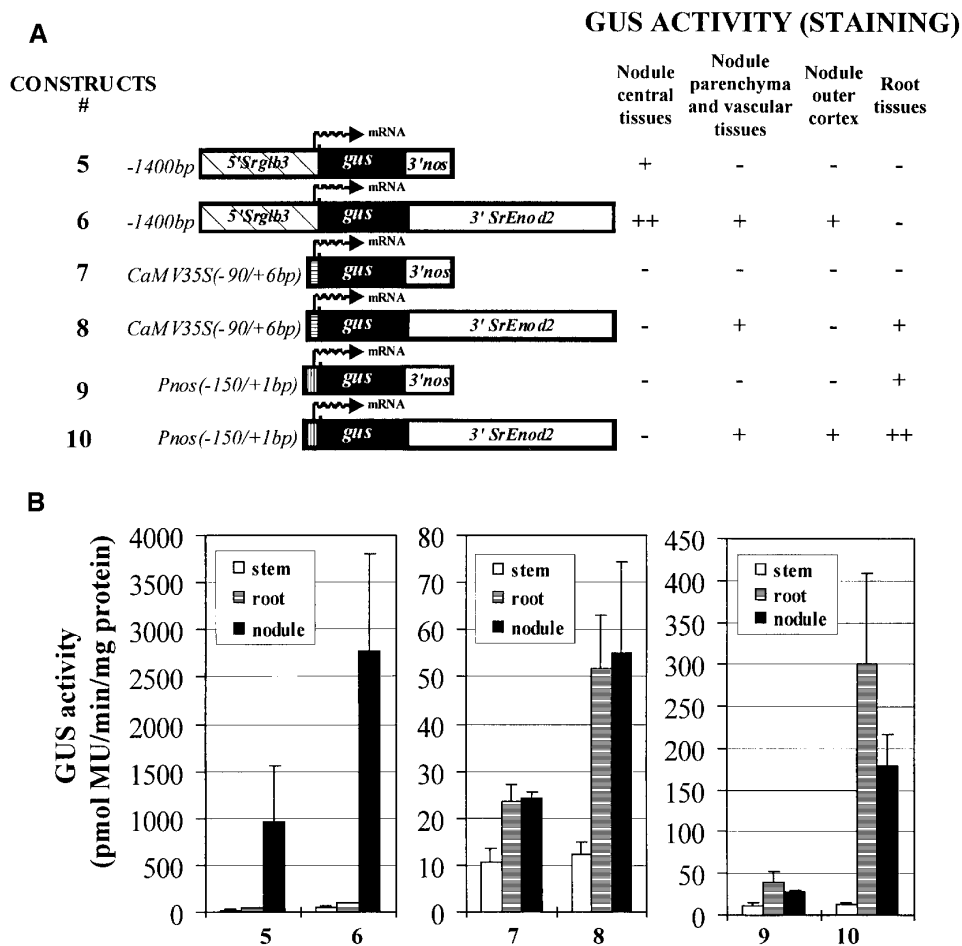
Figure 5. Structure of *gus* Fusion Constructs and Determination of GUS Activity in Transgenic *L. corniculatus* Plants.

(A) Structure of *gus* fusion constructs. The construct numbers are listed at left. The open boxes with diagonal lines represent the *S. rostrata* leghemoglobin gene promoter. The open boxes with horizontal lines represent the CaMV 35S minimal promoter (−90 to +6 bp). The open boxes with vertical lines represent the *nos* minimal promoter (*Pnos*, −150 to +1 bp). Other symbols are as described in the legend to Figure 2A.
(B) Quantification of GUS activity (picomoles of 4-methylumbelliferone [MU] per minute per milligram of protein) in transgenic *L. corniculatus* plants. The data represent the mean values. The error bars represent the standard deviation of the mean. Construct numbers are listed at the bottom.
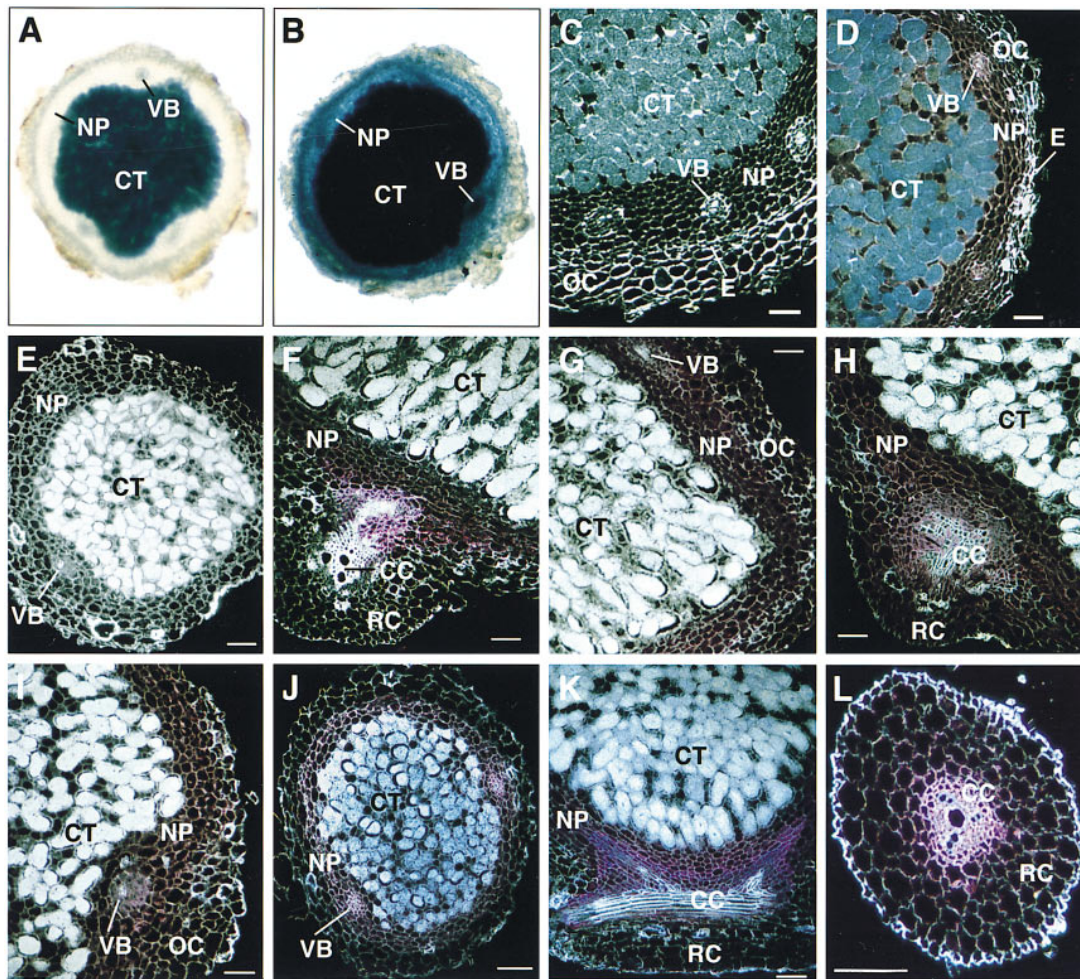
Figure 6. Microscopic Analysis of the Expression of *gus* Fusion Constructs in Transgenic *L. corniculatus* Plants.

Staining for GUS activity was conducted overnight (**[C]** to **[J]**) or for 1 hr (**[A]**, **[B]**, **[K]**, and **[L]**).

(A) Hand-cut section of a transgenic nodule harboring the 5′ *SrgIb*3–*gus*–3′ *nos* construct (Figure 5A, construct 5). GUS activity (blue color) can be seen in the nodule central tissue.

(B) Hand-cut section of a transgenic nodule harboring the 5′ *SrgIb*3–*gus*–3′ *SrEnod2* construct (Figure 5A, construct 6). GUS activity (blue color) can be seen in the nodule central tissue as well as in surrounding tissues.

(C) Dark-field microscopy of the nodule section shown in **(A)**. GUS activity (blue color) can be seen in the infected cells of the nodule central tissue.

(D) Dark-field microscopy of the nodule section shown in **(B)**. GUS activity (blue and brick-red colors) can be seen in the nodule central tissue as well as in the nodule parenchyma, vascular bundles, and outer cortical tissue.

(E) Dark-field microscopy of a transgenic nodule section harboring the 5′ CaMV 35S(−90/+6 bp)–*gus*–3′ *nos* construct (Figure 5A, construct 7).

(F) and **(G)** Dark-field microscopy of a proximal and a distal view, respectively, of a transgenic nodule section harboring the 5′ CaMV 35S(−90/+6 bp)–*gus*–3′ *SrEnod2* construct (Figure 5A, construct 8). GUS activity can be seen in the nodule parenchyma, vascular tissue bundles, and the root central cylinder. No GUS activity was observed in the root cortex.

(H) and **(I)** Dark-field microscopy of a proximal and a distal view, respectively, of a transgenic nodule section harboring the 5′ *Pnos*(−150/+1 bp)–*gus*–3′ *SrEnod2* construct (Figure 5A, construct 10). GUS activity can be seen in the nodule parenchyma, vascular bundles, and outer cortical tissue as well as in the root central cylinder and in the root cortex.

(J) Dark-field microscopy of a transgenic nodule section harboring the CaMV 35S(−150/−90 bp)–5′ *SrEnod2*(−115/+23 bp)–*gus*–3′ *SrEnod2* construct (Figure 8, construct 21). GUS activity can be seen in the nodule parenchyma, the nodule vascular bundles, and the nodule central tissue.

(K) and **(L)** Dark-field microscopy of nodule and root sections, respectively, from plants harboring the CaMV 35S(−150/−90 bp)–5′ *SrEnod2*(−50/+23)–*gus*–3′ *SrEnod2* construct (see Figure 8, construct 22). GUS activity can be seen in the nodule parenchyma, vascular bundles, and central tissue as well as in the root central cylinder and cortex.

CC, central cylinder; CT, central tissue; E, endodermis; NP, nodule parenchyma; OC, outer cortical tissue; RC, root cortex; VB, vascular bundle. Bars in **(C)** to **(L)** = 100 μm.

promoter and the *SrEnod2* 3′ region. In addition, the average expression level of the 5′ *Srglb3–gus*–3′ *SrEnod2* construct was consistently higher than that of the 5′ *Srglb3–gus*–3′ *nos* construct (Figure 5B).

The 5′ CaMV 35S(−90/+6)*–gus*–3′ *nos* construct (Figure 5A, construct 7) did not direct detectable levels of *gus* expression in either nodules or roots of transgenic plants (Figures 5A and 6E). However, when the 3′ *nos* terminator was replaced by the 3′ *SrEnod2* region (Figure 5A, construct 8), *gus* expression was detected in the nodule parenchyma, vascular bundles, and tissues surrounding the vascular bundle connecting the nodule to the root central cylinder (Figures 6F and 6G). *gus* expression also was detected in root vascular tissues but not in stems or leaves of transgenic plants (data not shown). Fluorometric measurements confirmed this observation (Figure 5B).

The *Pnos*(−150/+1 bp)*–gus*–3′ *nos* construct (where the *P* in *Pnos* stands for promoter; Figure 5A, construct 9) did not direct detectable levels of *gus* expression in nodules but was weakly expressed in the root tissues of transgenic plants (Figure 5B). Again, when the 3′ *nos* terminator was replaced by the 3′ *SrEnod2* region (Figure 5A, construct 10), *gus* expression could be detected readily in the nodule parenchyma, vascular bundles, and outer cortex as well as in root vascular tissues and cortical cells (Figures 6H and 6I). No staining was found in stems or leaves (data not shown). GUS activity measurement confirmed these observations (Figure 5B).

These data reveal that the 3′ region of the *SrEnod2* gene can extend the expression of the *gus* reporter gene to the parenchyma and vascular tissues of transgenic plants when fused to heterologous promoters, indicating that the *SrEnod2* 3′ region contains sequence determinants necessary and sufficient for directing reporter gene expression in the nodule parenchyma and vascular tissues.

Delimitation of Sequences in the 5′ Proximal Region of the *SrEnod2* Gene Required for Detectable Levels of Gene Expression

A series of 5′ to 3′ unidirectional deletions in the 5′ *SrEnod2* region was constructed and fused to the *gus* coding region as well as to the 3′ region of the *SrEnod2* gene (Figure 7A). The resulting constructs were introduced into *L. corniculatus* plants, and reporter gene expression was analyzed histochemically and quantitatively. GUS activity measurement revealed that constructs with deletions up to position −191, relative to the transcriptional start site mapped by Dehio and de Bruijn (1992), directed reporter gene expression in the same fashion as did the full-length 5′ *SrEnod2–gus*–3′ *SrEnod2* construct (Figure 2A, construct 1), namely, to the nodule parenchyma and vascular tissues (Figures 7A and 7B). Only the level of GUS activity varied slightly (Figure 7B). These data suggest that sequences up to position −191 (Figure 7A, construct 18) are not required for nodule paren-
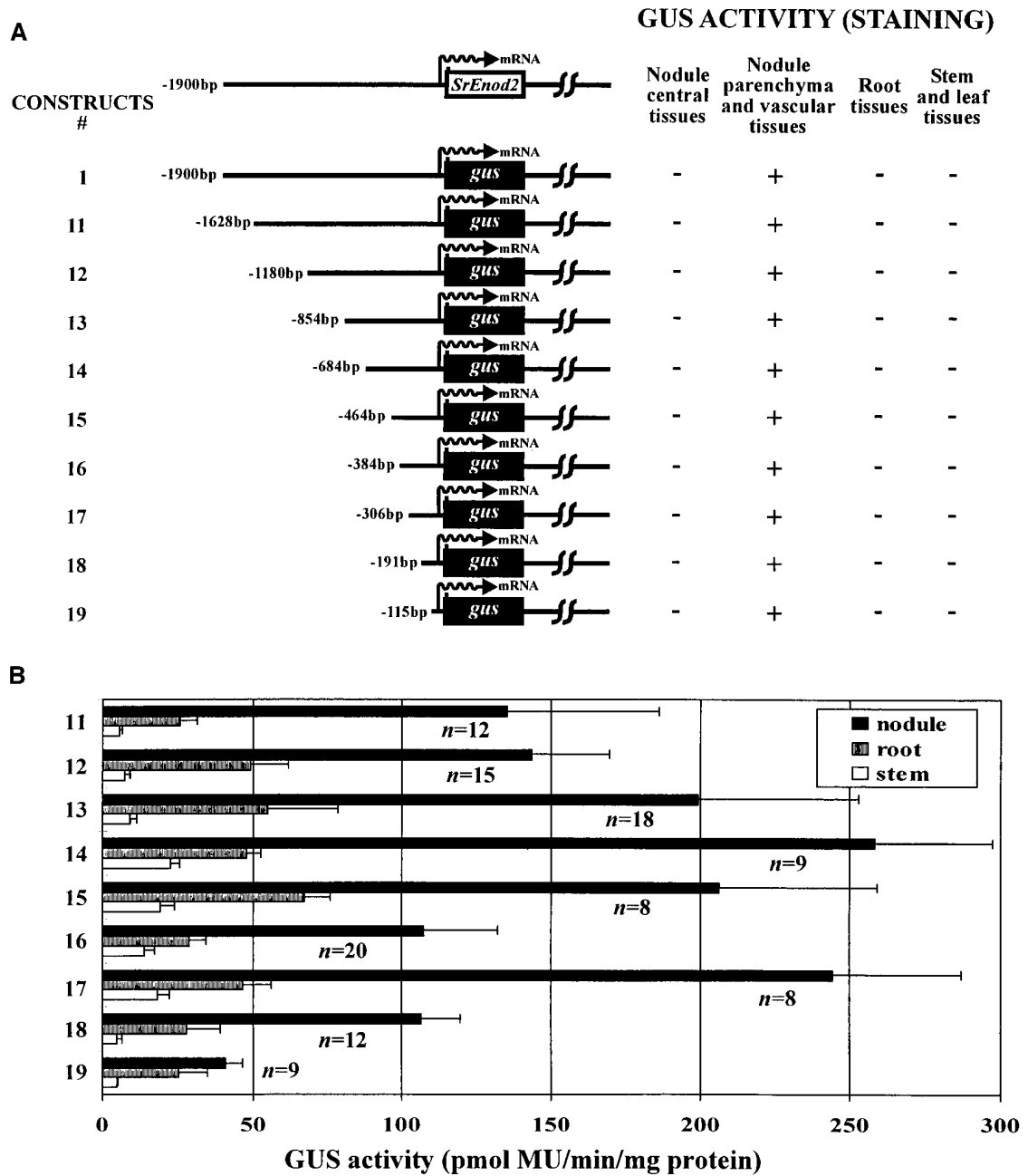
chyma–specific reporter gene expression. A deletion down to position −115 (Figure 7A, construct 19) was found to lead to a significant reduction of reporter gene expression in nodules (Figure 7B), although a limited degree of nodule-enhanced expression was maintained. Histochemical GUS staining revealed that this construct retained *gus* gene expression in the nodule parenchyma and vascular tissues (data summarized in Figure 7A). Therefore, we suggest that the sequences upstream of position −115 may not be absolutely necessary for nodule parenchyma–specific expression.

A construct with a deletion up to position −50 in the 5′ *SrEnod2* region was found to be inactive in transgenic plants (Figure 8, construct 20). To test whether the lack of reporter gene expression was due to a deletion of a tissue-specific *cis* element(s) or to a deletion of a proximal promoter element(s), we fused the transcriptional enhancer from the CaMV 35S promoter (−150 to −90 bp, part of domain B; Benfey et al., 1989) in *cis* to the −50-bp fragment (Figure 8, construct 22). GUS activity measurement in transgenic plants harboring this construct revealed that the reporter gene was expressed strongly in nodule, root, and stem tissues (Figure 8). Within nodules, the reporter gene was highly expressed in the nodule parenchyma and vascular tissues and at a lower level in the infected tissue (Figure 6K). Within roots, the *gus* gene was expressed in the central cylinder and cortical tissues (Figure 6L). When the same transcriptional enhancer was fused to the −115-bp deletion fragment of the 5′ *SrEnod2* gene (Figure 8, construct 21), a GUS activity staining pattern identical to that of construct 22 (Figures 6K, 6L, and 8) was observed, although GUS activity was much lower than in plants harboring construct 22 (Figure 6J; data summarized in Figure 8). These data suggest that sequences between positions −115 and −50 in the 5′ *SrEnod2* region are necessary for reporter gene expression. However, they may not contain any tissue-specific *cis* elements.

The 3′ UTR of the *SrEnod2* Gene Constitutes the Minimum Determinant for Nodule Parenchyma–Specific Gene Expression

To delineate the sequence determinants in the 3′ region of the *SrEnod2* gene responsible for nodule parenchyma–specific expression, we constructed a series of 3′ to 5′ unidirectional deletions in the 3′ region of the *SrEnod2* gene (Figure 9A). The 3′ deletion derivatives were fused to the *gus* coding region flanked by the full-length 5′ *SrEnod2* region. The resulting constructs were introduced into *L. corniculatus*, and reporter gene expression was determined. As shown in Figure 9B, deletions in the 3′ region up to position +400 bp relative to the stop codon (Figure 9A, construct 29) did not affect tissue-specific expression of the reporter gene. The level of gene expression was reduced greatly when the 3′ flanking sequences were further limited to position +241 bp, although the nodule parenchyma–specific expression pattern

A

GUS ACTIVITY (STAINING)

CONSTRUCTS #		Nodule central tissues	Nodule parenchyma and vascular tissues	Root tissues	Stem and leaf tissues
	-1900bp SrEnod2				
1	-1900bp gus	-	+	-	-
11	-1628bp gus	-	+	-	-
12	-1180bp gus	-	+	-	-
13	-854bp gus	-	+	-	-
14	-684bp gus	-	+	-	-
15	-464bp gus	-	+	-	-
16	-384bp gus	-	+	-	-
17	-306bp gus	-	+	-	-
18	-191bp gus	-	+	-	-
19	-115bp gus	-	+	-	-

B

GUS activity (pmol MU/min/mg protein)

Figure 7. Structure of 5′ Deletion Constructs and GUS Activity in Transgenic *L. corniculatus* Plants.

(A) Structure of *gus* fusion constructs. The construct numbers are listed at left. The numbers in base pairs indicate the end point of the 5′ deletion relative to the start of transcription. The short vertical bars attached to the boxes represent the translational start of the corresponding genes. The interrupted lines downstream of the *gus* reporter gene represent the 2.4-kb 3′ flanking sequences of the *SrEnod2* gene. For other designations, see the legend to Figure 2A.

(B) Quantification of GUS activity (picomoles of 4-methylumbelliferone [MU] per minute per milligram of protein) in transgenic *L. corniculatus* plants. The data represent the mean values. The error bars represent the standard deviation of the mean. *n* indicates the number of transgenic plants tested. Construct numbers are listed at left.

appeared to be maintained (Figure 9A, construct 30; data not shown). Therefore, the 241-bp fragment immediately downstream of the stop codon of the *SrEnod2* gene appears to be sufficient to direct gene expression to the nodule parenchyma and vascular tissues. This 241-bp fragment contains most of the *SrEnod2* 3′ untranslated sequence because the poly(A) addition site is located between positions 256 and 258 (Dehio and de Bruijn, 1992; Chen, 1996).

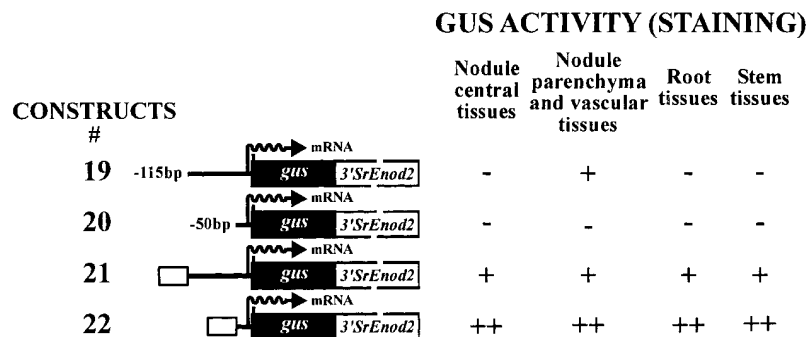## The 3′ UTR of the *SrEnod2* Gene Does Not Function as a Transcriptional Enhancer Element

To investigate the potential mode of action of the *SrEnod2* 3′ UTR element, we inserted a fragment carrying 400 bp of 3′ UTR sequences (see Figure 9A, construct 29) in both orientations in front of a 684-bp 5′ fragment (see Figure 7, construct 14) fused to the *gus* reporter gene and the 3′ *nos* terminator (Figure 10, constructs 33 and 34). As controls, constructs were made containing the same 684-bp 5′ fragment fused to the *gus* reporter gene and the 400-bp *SrEnod2* 3′ UTR or the 3′ *nos* terminator (Figure 10, constructs 31 and 32, respectively). These constructs were introduced into *L. corniculatus* plants, and GUS activity was analyzed in different tissues of the transgenic plants by GUS staining. The results are summarized in Figure 10. Although the positive control construct 31 was found to display the typical nodule parenchyma– and vascular bundle–specific expression pattern, neither of the chimeric constructs containing the *SrEnod2* 3′ UTR fused to the *SrEnod2* 5′ (promoter) region and the *nos* terminator displayed any detectable GUS activity (Figure 10, constructs 33 and 34). Therefore, the *SrEnod2* 3′ UTR does not act as a transcriptional enhancer.

DISCUSSION

The 3′ UTR of *SrEnod2* Confers Nodule Parenchyma–Specific Expression
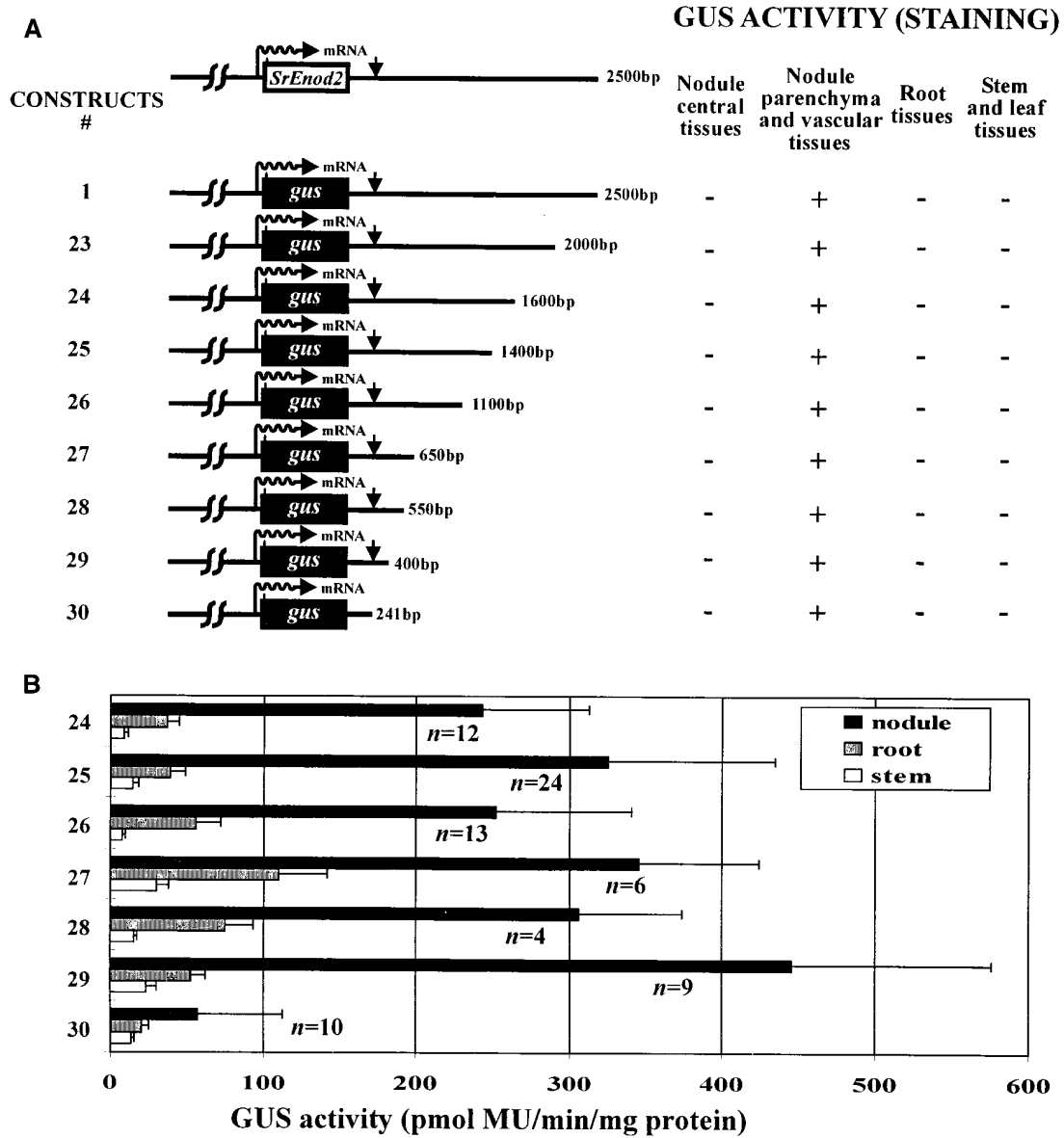
The *Enod2* genes of several legumes have been shown to be expressed in the nodule parenchyma cell layer (Van de Wiel et al., 1990a, 1990b; Allen et al., 1991; Figure 1). Here, we show that in the case of the tropical legume *S. rostrata*, the primary determinant of this cell-specific expression pattern is located in the 3′ UTR of the *SrEnod2* gene. The following lines of evidence support this conclusion: (1) Chimeric *gus* reporter constructs flanked by both 5′ and 3′ regions of the *SrEnod2* gene are expressed in the parenchyma of transgenic *L. corniculatus* nodules, whereas constructs containing a heterologous 3′ region (e.g., 3′ *nos*) are not (Figures 2 and 3). (2) The presence of the *SrEnod2* 3′ region is necessary for the accumulation of the *gus* mRNA in transgenic nodules (Figure 4). (3) The addition of the *SrEnod2* 3′ region to chimeric reporter gene constructs containing different heterologous promoters (e.g., *Srglb*3 promoter, CaMV 35S minimal promoter, and *nos* minimal promoter) extends the expression pattern normally observed with these promoters to the nodule parenchyma in a similar fashion, regardless of the promoter used (Figure 5).

One interesting observation during our analysis of *gus* reporter gene expression was that all of the *gus* constructs containing the *SrEnod2* 3′ region directed *gus* expression to the vascular bundles of transgenic *L. corniculatus* nodules as well. This observation is in contrast with our in situ hybridization results (Figure 1), which did not reveal *SrEnod2* mRNA accumulation in the vascular bundles. It also is in contrast with previous results from soybean *Enod2* gene/promoter expression analyses, which did not reveal reporter

GUS ACTIVITY (STAINING)

CONSTRUCTS #		Nodule central tissues	Nodule parenchyma and vascular tissues	Root tissues	Stem tissues
19	-1i5bp ▬ [gus] [3'SrEnod2]	−	+	−	−
20	-50bp ▬ [gus] [3'SrEnod2]	−	−	−	−
21	☐— [gus] [3'SrEnod2]	+	+	+	+
22	☐— [gus] [3'SrEnod2]	++	++	++	++

Figure 8. Structure of 5′ Deletion Constructs/Enhancer Fusions and GUS Activity in Transgenic *L. corniculatus* Plants.

The construct numbers are listed at left. The numbers in base pairs indicate the end point of the 5′ deletions relative to the start of transcription. The interrupted open boxes represent the 2.4-kb 3′ flanking region of the *SrEnod2* gene. The open boxes represent the transcriptional enhancer of the CaMV 35S promoter (−150 to −90 bp). For other designations, see the legend to Figure 2A.

A

GUS ACTIVITY (STAINING)

CONSTRUCTS #		Nodule central tissues	Nodule parenchyma and vascular tissues	Root tissues	Stem and leaf tissues
	SrEnod2 mRNA 2500bp				
1	*gus* mRNA 2500bp	−	+	−	−
23	*gus* mRNA 2000bp	−	+	−	−
24	*gus* mRNA 1600bp	−	+	−	−
25	*gus* mRNA 1400bp	−	+	−	−
26	*gus* mRNA 1100bp	−	+	−	−
27	*gus* mRNA 650bp	−	+	−	−
28	*gus* mRNA 550bp	−	+	−	−
29	*gus* mRNA 400bp	−	+	−	−
30	*gus* mRNA 241bp	−	+	−	−

B

GUS activity (pmol MU/min/mg protein)

Figure 9. Structure of 3′ Deletion Constructs and Determination of GUS Activity in Transgenic *L. corniculatus* Plants.

(A) Structure of *gus* fusion constructs. The construct numbers are listed at left. The numbers in base pairs indicate the end points of the 3′ deletions relative to the stop codon of the *SrEnod2* gene. The interrupted lines at the 5′ end represent the 1.9-kb 5′ *SrEnod2* region. The short vertical bars attached to the boxes represent the translational start of the corresponding genes. The vertical arrows indicate the position of the polyadenylation site(s) of the *SrEnod2* gene (Dehio and de Bruijn, 1992; Chen, 1996). Other designations are as given in the legend to Figure 2A. **(B)** Quantification of GUS activity (picomoles of 4-methylumbelliferone [MU] per minute per milligram of protein) in transgenic plants. The data represent the mean values. The error bars represent the standard deviation of the mean. *n* indicates the number of transgenic plants tested. Construct numbers are listed at left.

GUS ACTIVITY (STAINING)

CONSTRUCTS #		Nodule central tissues	Nodule parenchyma and vascular tissues	Root tissues	Stem and leaf tissues
31 (3)	5'SrEnod2 gus 3'SrEnod2	-	+	-	-
32 (7)	5'SrEnod2 gus 3'nos	-	-	-	-
33 (3)	3'SrEnod2→ 5'SrEnod2 gus 3'nos	-	-	-	-
34 (12)	←3'SrEnod2 5'SrEnod2 gus 3'nos	-	-	-	-

Figure 10. Structure of Chimeric Constructs Containing the *SrEnod2* 3′ UTR Fused to the *SrEnod2* Promoter Region in *cis* and GUS Activity in Transgenic *L. corniculatus* Plants.

The construct numbers are listed at left, and the number of transgenic plants analyzed is in parentheses. The arrows in the 3′ *SrEnod2* boxes indicate the direction of the fusion. For other designations, see the legend to Figure 2A. For construction details, see the text.

gene expression in the vascular tissues either (Lauridsen et al., 1993). Although we cannot formally rule out the possibility that the observed *gus* expression in the nodule vascular bundles is due to an artifact, we have observed that positive GUS staining first occurred in the nodule vascular tissues and subsequently in the parenchyma cells rather than in the opposite order. This observation argues against artifacts caused by the diffusion of the GUS enzyme or its colored product and suggests instead that the GUS staining pattern reported here does reflect true gene expression. Consistent with the hypothesis that the *S. rostrata Enod2* gene differs from the soybean homolog, the *S. rostrata Enod2* gene is inducible by cytokinin (Dehio and de Bruijn, 1992; Silver et al., 1996), whereas the soybean *Enod2* gene is not. Moreover, in the case of the soybean *Enod2* gene, nodule parenchyma–specific expression has been reported to be controlled by elements far upstream in the 5′ region of the gene (Lauridsen et al., 1993; also see below).

Another interesting observation was made with the chimeric 5′ *Srglb3–gus*–3′ *SrEnod2* construct. We found that the *SrEnod2* 3′ region and the *Srglb3* promoter have additive effects on cell specificity, because the *gus* reporter gene was expressed in both the nodule parenchyma/vascular bundles and the infected cells of the central tissue (Figure 6D). In addition, the *gus* gene also was expressed in the central uninfected cells. This unexpected expression pattern may be due to an unusual interaction of the *cis*-acting elements in these 5′ and 3′ regions. Alternatively, because the results shown in Figure 6 suggest that the *SrEnod2* 3′ region appears to confer both a tissue-specific as well as a quantitative function(s), it may reflect a stimulation of *Srglb3* promoter activity in the uninfected cells to a previously undetectable level (Szczyglowski et al., 1994).

Our *SrEnod2* 3′ deletion analysis revealed that the DNA sequences downstream of position +400 bp, relative to the

SrEnod2 stop codon, can be omitted without affecting the expression pattern of chimeric reporter gene constructs (Figure 9). In fact, even a deletion construct lacking DNA sequences 3′ to position +241 directs expression to the nodule parenchyma, whereas expression in roots, stems, and leaves is virtually undetectable (Figure 9). This suggests that sequences between the *SrEnod2* stop codon and position +241, upstream of the poly(A) addition site (positions +256 to +258; Dehio and de Bruijn, 1992; Chen, 1996), are capable of directing cell-specific expression in transgenic nodules, albeit at a low level.

DNA elements in the 3′ region of plant genes have been implicated previously in regulation of gene expression. Examples include the potato proteinase inhibitor II gene (Thornburg et al., 1987; An et al., 1989), the petunia ribulose bisphosphate carboxylase small subunit gene (Dean et al., 1989), the oilseed rape *AX92* gene (Dietrich et al., 1992), the Arabidopsis *GLABROUS1* gene (Larkin et al., 1993), and the potato sucrose synthase genes (Fu et al., 1995a, 1995b). Multiple examples have also been reported in mammalian systems. Examples include the chicken adult β-globin gene (Choi and Engel, 1986), the chicken histone *H5* gene (Trainor et al., 1987), the human *A*γ globin gene (Bodine and Ley, 1987), the mammalian ribonucleotide reductase *R1* gene (Chen et al., 1993), and the human transferrin receptor gene (Owen and Kuhn 1987; Binder et al., 1994). In these cases, the 3′ sequences act either as transcriptional enhancers or as sequence determinants modulating gene expression post-transcriptionally. The *cis* element(s) acting as a transcriptional enhancer generally is located downstream of the poly(A) addition site(s) and often acts as a tissue-specific and/or developmental regulatory element(s) (e.g., the Arabidopsis *GLABROUS1* gene, chicken adult β-globin gene, chicken histone *H5* gene, and human *A*γ globin gene). In those cases in which post-transcriptional regulation is in-

volved, the 3′ sequences modulate mRNA stability (petunia small subunit ribulose bisphosphate carboxylase gene and human transferrin receptor gene) or efficacy of mRNA 3′ end formation and processing (potato proteinase inhibitor II gene). In addition, different 3′ end regions also have been found to influence the level of gene expression in plant cells (Ingelbrecht et al., 1989).

However, our finding that the *cis* element(s) responsible for cell-specific expression is located within the 3′ UTR appears to be a unique example among plant nuclear genes. The mechanism by which the *SrEnod2* 3′ UTR mediates nodule parenchyma–specific expression remains to be elucidated. In a separate but related study, we have shown that cytokinin-mediated enhancement of *SrEnod2* gene expression in *S. rostrata* roots, in the absence of infection with rhizobia, appears to occur post-transcriptionally (Silver et al., 1996). This aspect of *SrEnod2* regulation also involves the 3′ UTR of the gene (Silver, 1996). However, we postulate that a post-transcriptional mechanism may be involved in tissue-specific gene expression mediated by the *SrEnod2* 3′ UTR as well, because the *SrEnod2* 3′ UTR element failed to act as a transcriptional enhancer when fused to the *SrEnod2* promoter in *cis* (Figure 10).

Whether nodule parenchyma–specific expression and cytokinin upregulation of the *SrEnod2* gene share common regulatory elements currently is not known, and several potential mechanisms, including interaction of the 3′ UTR with promoter elements to enhance transcription in nodule parenchyma cells, can be postulated. Cell-specific mRNA stability elements have been identified in the 3′ UTR of the α2 globin gene (Weiss and Liebhaber, 1995). It is possible that the *SrEnod2* 3′ UTR directs nodule parenchyma–specific expression in a manner similar to the 3′ UTR of the α2 globin gene.

The 5′ Region of *SrEnod2* Does Not Appear to Harbor Significant Tissue-Specific *cis* Elements

Our deletion analysis of the *SrEnod2* 5′ region revealed that sequences upstream of position −191, relative to the transcriptional start site, are not required for nodule parenchyma–specific expression. A deletion up to the −50-bp position abolishes reporter gene expression in nodules, but fusing a transcriptional enhancer (CaMV 35S −150 to −90 bp; see Szabados et al., 1990) to the −50-bp fragment restores reporter gene expression to the nodule parenchyma/vascular tissue, to stem and root tissues, and to a limited extent to the nodule central tissue (Figure 6K). This pattern of reporter gene expression was found to be similar to the pattern directed by a fusion of the same transcriptional enhancer to the −115-bp fragment of the *SrEnod2* 5′ region (Figure 6J). These data suggest that sequences between positions −115 and −50 are required for a significant level of reporter gene expression in nodules. However, these sequences are not likely to contain a nodule tissue–specific *cis* element(s).

The latter conclusion is very intriguing in light of the fact that in the case of the soybean *Enod2B* gene, Lauridsen et al. (1993) have reported that the 3-kb promoter region directed reporter gene expression to the parenchyma of *L. corniculatus* and *Trifolium repens* transgenic hairy root nodules. The 3′ *nos* terminator was used in their study. Two critical tissue-specific *cis* elements were identified in regions located between positions −1792 and −1582 and between −380 and −53 that were relative to the transcriptional start site of the soybean *Enod2B* gene. When the upstream tissue-specific *cis* element was fused to the promoter region of a leghemoglobin gene (*lb*), the resulting gene fusion was found to direct a low level of reporter gene expression in a scattered pattern in the nodule central area. These data appear to contradict the data presented in this study and/or to suggest further that there are profound differences in the mechanisms regulating *SrEnod2* and soybean *Enod2B* gene expression (also see the discussion above).

Additional support for this concept is the finding that DNA sequences in the promoter regions of the *SrEnod2* and the soybean *Enod2B* genes share remarkably little homology (de Bruijn et al., 1994), in contrast to the late-nodulin *lb* promoters, which are highly similar (Stougaard et al., 1987; de Bruijn et al., 1990; Szabados et al., 1990; de Bruijn and Schell, 1992; Ramlov et al., 1993; Szczyglowski et al., 1994). Perhaps this discrepancy can be explained once the nucleotide sequences of the *cis* element(s) responsible for the nodule parenchyma–specific gene expression are identified and compared directly. Whatever the case may be, the apparent involvement of the 3′ region of the *SrEnod2* gene, rather than its promoter (5′) region, in nodule parenchyma–specific expression is unique in a variety of ways and opens up a whole new area of investigations into the mechanisms of plant gene expression in response to rhizobial infection.

METHODS

Plant Growth and Nodulation

Sesbania rostrata seeds were surface-sterilized and germinated on Petri dishes in the dark at 28°C for 1 day, as described by Pawlowski et al. (1991). Seedlings were grown for 3 weeks in autoclaved soil mix (MetroMix [Scotts-Sierra Horticultural Products, Marysville, OH]/sand; 2:1) in growth chambers with an 18-hr-light (28°C) and 6-hr-dark (22°C) cycle. Plants were inoculated with a 2-day-old culture of *Azorhizobium caulinodans* ORS571 (Dreyfus and Dommergues, 1981) either in pots for root nodulation or on stems for stem nodulation. Six-day-old root nodules and stem nodules were collected and processed (see below).

Transgenic *Lotus corniculatus* plants were grown for 1 week in autoclaved soil mix (vermiculite/sand/MetroMix; 10:10:1) in growth chambers with a 16-hr-light (24°C) and 8-hr-dark (18°C) cycle. Plants were inoculated with a 3-day-old culture of *Rhizobium loti* NZP2037 (Pankhurst et al., 1983) and grown for 21 days. Plant tissues (nodules, infected roots, and leaves plus stems) were collected and

stained for β-glucuronidase (GUS) activity or stored in liquid nitrogen for GUS activity quantification.

In Situ RNA Localization

In situ RNA localization studies were conducted essentially as described by Cox and Goldberg (1988) and Van de Wiel et al. (1990a), except that a nonradioactive approach was used according to De Block and DeBrouwer (1993). Stem and root nodules were fixed in 10 mM sodium phosphate buffer, pH 6.8, containing 4% paraformaldehyde, 0.25% glutaraldehyde, and 100 mM NaCl at room temperature, dehydrated in a graded ethanol and xylene series, and embedded in Paraplast X-tra (Fisher Scientific, Pittsburgh, PA). Nodule sections (7 μm thick) were cut and attached to Superfrost/plus microscopic slides (Fisher Scientific). After removal of the paraplast with xylene and rehydration through an ethanol series, sections were treated with proteinase K (5 mg/mL) in 100 mM Tris-HCl, pH 7.5, and 50 mM EDTA for 30 min at 37°C and with 0.25% acetic anhydride in 100 mM triethanolamine, pH 8.0, for 10 min at room temperature. Slides were subsequently dehydrated through an ethanol series and dried and hybridized with digoxigenin-labeled sense and antisense RNA probes generated by transcribing the coding region of the *S. rostrata* early nodulin *SrEnod2* gene (Dehio and de Bruijn, 1992) with T3 and T7 RNA polymerase, according to the manufacturer's instructions (Boehringer Mannheim).

Hybridization and washing were essentially performed according to Cox and Goldberg (1988) and De Block and DeBrouwer (1993). Sections were dehydrated via an ethanol series and mounted with Polymount (Polysciences Inc., Warrington, PA). Sections were photographed using an Axiophot microscope (Zeiss, Oberkochen, Germany).

Isolation of Total RNA and Poly(A)+ RNA

Total RNA was isolated according to the hot phenol method of Verwoerd et al. (1989), with the following modifications. Briefly, plant material (up to 1 gm) was ground in liquid nitrogen to a fine powder and then transferred into a 15-mL tube containing 4 mL of preheated (65°C) RNA isolation buffer (Hall et al., 1978) and 4 mL of preheated (65°C) phenol. Samples were vortexed vigorously for 5 min, 4 mL of chloroform was added, and the mixture was vortexed again for 15 min and centrifuged at 10,000 rpm for 20 min. The supernatant was extracted once with an equal volume of chloroform and centrifuged again. RNA in the supernatant was precipitated at 10,000 rpm for 30 min after adding one-quarter volume of 8 M LiCl and one-tenth volume of 1.6 M KCl and after an overnight incubation on ice. The RNA pellet was resuspended in 400 μL of diethyl pyrocarbonate (DEPC)–treated water and extracted with an equal volume of chloroform until a clear interface was formed. RNA was then precipitated and resuspended in DEPC–H_2O. The RNA concentration was determined photometrically.

Poly(A)+ RNA was prepared by passing total RNA through oligo(dT) columns, according to the manufacturer's instructions (5′ to 3′, Boulder, CO). RNA gel blot analysis was performed according to standard procedures (Maniatis et al., 1989). Briefly, Poly(A)+ RNA was loaded on a 1% formaldehyde agarose gel and separated at 4°C. The gel was soaked in 10 × SSC (1 × SSC contains 0.15 M NaCl and 0.015 M sodium citrate) for 30 min to remove formaldehyde and subsequently blotted to a 0.22-μm nitrocellulose membrane (NitroPlus; Micron Separation Inc., Westborough, MA). The membrane was rinsed briefly in DEPC-treated water and baked at 80°C for 2 hr

under vacuum. Prehybridization was conducted at 51°C overnight in a solution containing 5 × SSC, 10 × Denhardt's solution (Maniatis et al., 1989), 0.1% SDS, 0.1 M KPO_4, pH 6.8, and 100 μg/mL salmon sperm DNA. Hybridization reactions were performed at 65°C for 18 hr in a solution containing 1 × SSC, 10 × Denhardt's solution, 0.1 M KPO_4, pH 6.8, 100 μg/mL salmon sperm DNA, 10% dextran sulfate, and 50% formamide. After hybridization, the membrane was washed at 65°C in 2 × SSC and 1 × SSC for 20 min each and finally in 0.2 × SSC for 40 min. Blots were exposed to x-ray film at −75°C.

Chimeric Reporter Gene Construction

A 5.3-kb EcoRI fragment, which contains a 1.9-kb 5′ region, a 1-kb coding region, and a 2.4-kb 3′ downstream region of the *SrEnod2* gene, was subcloned from the genomic clone λCD1 (Dehio and de Bruijn, 1992) into the pBluescript KS− vector (Stratagene, La Jolla, CA). Restriction sites (BamHI and SalI) were introduced at the translational initiation codon and at the 3′ end of the putative signal peptide sequence of the *SrEnod2* gene by using site-directed mutagenesis, as described by Kunkel (1985). The oligonucleotide primers used for introducing the BamHI and SalI sites were 5′-GAGTAGTGTAGA-GAGGA**TCC**TTCTATCTAT-3′ and 5′-GGCTCATAGTAATTAG**TCG**AC-ACTGGAG-3′, respectively. The underlined nucleotide sequences correspond to the restriction endonuclease recognition sites, and the boldface nucleotides correspond to the mutations introduced.

A 1.9-kb EcoRI-BamHI fragment, which contains the entire 5′ untranslated region (UTR) and upstream region of the *SrEnod2* gene, was inserted in front of the *gus* coding region carried on plasmid pBI101.1 (Clontech Laboratories, Palo Alto, CA). The EcoRI end of the fragment was filled in with the Klenow fragment of DNA polymerase I before cloning. The resulting binary vector was used to generate constructs 1 and 2 (Figure 2A).

To construct a transcriptional fusion between the 1.98-kb 5′ sequences of the *SrEnod2* gene and the *gus* coding region, we performed second-round mutagenesis with the 5.3-kb EcoRI fragment containing the introduced SalI site with an oligonucleotide carrying a mutation in the translational initiation codon (ATG to GGA). The resulting 1.98-kb EcoRI-(BamHI)-SalI fragment was excised and inserted in front of the *gus* coding region carried on plasmid pBI101.1. This vector was used to generate constructs 3 and 4 (Figure 2A).

A restriction site (SacI; underlined and boldface) was introduced immediately downstream of the translational stop codon (TAA) of the *SrEnod2* gene by using the oligonucleotide primer 5′-GTAGTG-GTAGTGGTTG**GAGCTC**TTAATTTTTTTTTGG-3′. A 2.4-kb SacI-EcoRI fragment, containing the entire 3′ untranslated and downstream region of the *SrEnod2* gene, was inserted into pBI101.1 to generate constructs 1 and 3 (Figure 2A).

Constructs 5 and 6 were generated by inserting a 3.4-kb HindIII-SacI fragment of plasmid pLP14 (Szczyglowski et al., 1994), containing a 1.4-kb 5′ sequence of the *Srglb3* gene and the *gus* coding region, into pBI101.1 and pBI101-3′ *SrEnod2*, respectively. Constructs 7, 8, 9, and 10 were generated in a similar fashion by inserting into the BamHI-SacI sites of pBI101.1 and pBI101-3′ *SrEnod2* a 2.1-kb BamHI-SacI fragment of pLP70, containing the 96-bp minimal cauliflower mosaic virus (CaMV) 35S promoter (−90 to +6 bp) and the *gus* coding region, and a 2.15-kb BamHI-SacI fragment of pLP62, containing the 150-bp minimal nopaline synthase (*nos*) promoter (−150 to +1 bp) and the *gus* coding region, respectively.

Several 5′ deletion fragments were generated by restriction enzyme digestion of the 1.9-kb EcoRI-BamHI fragment. XbaI, Sau3A,

RsaI, EcoRV, DraI, MspI, HinfI, AluI, SspI, and Tsp were used to generate deletions ending at positions −1628, −1180, −854, −684, −464, −384, −306, −191, −115, and −50 bp, respectively, relative to the transcriptional start point. Several 3′ deletion fragments were generated by nested deletions, using the Erase-a-Base kit (Promega). A XhoI linker was inserted into the EcoRI site at the end of the 3′ sequences of the *SrEnod2* gene in construct 1. The 3′ deletion fragments were then inserted into the SacI-XhoI sites of the modified construct 1.

In construct 31, the *gus* reporter gene was fused to a 684-bp 5′ *SrEnod2* (promoter) fragment and a 400-bp 3′ *SrEnod2* 3′ UTR fragment, respectively (Figure 10). In construct 32, the *gus* reporter gene was fused to the same 684-bp 5′ *SrEnod2* fragment but was flanked with the 3′ *nos* terminator fragment. Constructs 33 and 34 were directly derived from construct 32 by inserting the *SrEnod2* 400-bp 3′ UTR fragment in front of the *SrEnod2* promoter region in both orientations (Figure 10).

Regeneration of Transgenic *L. corniculatus* Plants

Transgenic plants (*L. corniculatus* cv Rodeo) were generated according to Szabados et al. (1990). Binary vectors were conjugally transferred into *Agrobacterium rhizogenes* A4 (Tempe and Casse-Delbart, 1989). Regenerated plants were transferred to a growth chamber (Conviron, Asheville, NC) and nodulated as described previously (Szabados et al., 1990).

Quantification of GUS Activity

GUS activity was quantified according to Jefferson et al. (1987). The units of GUS activity used were picomoles of 4-methylumbelliferone produced per minute per milligram of protein. The concentration of protein in the extract was determined by the Bradford assay (Bradford, 1976). Fluorometric assays were performed using a fluorescence spectrophotometer (model F-2000; Hitachi, Tokyo, Japan).

Histochemical Staining of GUS Activity

GUS activity was analyzed histochemically according to the procedure described by Jefferson (1987), with the following modifications. Hand-cut nodule sections were incubated at 37°C in a solution containing 50 mM Na_2PO_4 and $NaHPO_4$, pH 7, 1 mM ferricyanide and ferrocyanide, 20% methanol, and 1 mM 5-bromo-4-chloro-3-indolyl β-D-glucuronide (Gold Biotechnology Inc., St. Louis, MO). Stained sections were then embedded in historesin (Reichert-Jung; Cambridge Instruments, Heidelberg, Germany), as described by De Block and DeBrouwer (1992), or in Paraplast X-Tra, as described by Cox and Goldberg (1988). Sections (10 μm thick) were generated and examined by dark- and light-field microscopy by using an Axiophot microscope.

REFERENCES

Allen, T., Raja, S., and Dunn, K. (1991). Cells expressing Enod2 show differential spatial organization during the development of alfalfa root nodules. Mol. Plant-Microbe Interact. **2,** 139–146.

An, G., Mitra, A., Choi, H.K., Costa, M.A., An, K., Thornburg, R.W., and Ryan, C.A. (1989). Functional analysis of the 3′ control region of the potato wound-inducible proteinase inhibitor II gene. Plant Cell **1,** 115–122.

Arora, N., Skoog, F., and Allen, O.N. (1959). Kinetin-induced pseudonodules on tobacco roots. Am. J. Bot. **46,** 610–613.

Averyhart-Fullard, V., Datta, K., and Marcus, A. (1988). A hydroxyproline-rich protein in the soybean cell wall. Proc. Natl. Acad. Sci. USA **85,** 1082–1085.

Benfey, P.N., Ren, L., and Chua, N.-H. (1989). The CaMV 35S enhancer contains at least two domains which can confer developmental and tissue-specific expression patterns. EMBO J. **8,** 2195–2202.

Binder, R., Horowitz, J.A., Basilion, J.P., Koeller, D.M., Klausner, R.D., and Harford, J.B. (1994). Evidence that the pathway of transferrin receptor mRNA degradation involves an endonucleolytic cleavage within the 3′ UTR and does not involve poly(A) tail shortening. EMBO J. **13,** 1969–1980.

Bodine, D.M., and Ley, T.J. (1987). An enhancer element lies 3′ to the human Aγ globin gene. EMBO J. **6,** 2997–3004.

Bradford, M.M. (1976). A rapid and sensitive method for the quantitation of microgram quantities of protein utilizing the principle of protein–dye binding. Anal. Biochem. **72,** 248–254.

Chen, F.Y., Amara, F.M., and Wright, J.A. (1993). Mammalian ribonucleotide reductase R1 mRNA stability under normal and phorbol ester stimulating conditions: Involvement of a *cis-trans* interaction at the 3′ untranslated region. EMBO J. **12,** 3977–3986.

Chen, R. (1996). Structure, Function and Regulation of Early Nodulin Gene *Enod2* from Legume Plants. PhD Dissertation (East Lansing, MI: Michigan State University).

Choi, O.-R., and Engel, J.D. (1986). A 3′ enhancer is required for temporal and tissue-specific transcriptional activation of the chicken adult β-globin gene. Nature **323,** 731–734.

Cooper, J.B., and Long, S.R. (1994). Morphogenetic rescue of *Rhizobium meliloti* nodulation mutants by *trans*-zeatin secretion. Plant Cell **6,** 215–225.

Cox, K.H., and Goldberg, R.B. (1988). Analysis of plant gene expression. In Plant Molecular Biology: A Practical Approach, C.H. Shaw, ed (Oxford, UK: IRL Press), pp. 1–34.

Dean, C., Favreau, M., Bond-Nutter, D., Bedbrook, J., and Dunsmuir, P. (1989). Sequences downstream of translation start regulate quantitative expression of two petunia *rbcS* genes. Plant Cell **1,** 201–208.

De Block, M., and DeBrouwer, D. (1992). *In-situ* enzyme histochemistry on plastic embedded plant material: The development of an artifact-free β-glucuronidase assay. Plant J. **2,** 261–266.

De Block, M., and DeBrouwer, D. (1993). RNA–RNA *in-situ* hybridization using digoxigenin labeled probes: The use of high molecular weight polyvinylalcohol in the alkaline phosphatase indoxyl-nitroblue-tetrazolium reaction. Anal. Biochem. **215,** 86–89.

de Bruijn, F.J. (1989). The unusual symbiosis between the diazotrophic stem-nodulating bacterium *Azorhizobium caulinodans* ORS571 and its host, the tropical legume *Sesbania rostrata.* In Plant–Microbe Interactions: Molecular and Genetic Perspectives, Vol. 3, T. Kosuge and E. Nester, eds (New York: McGraw Hill), pp. 457–504.

de Bruijn, F.J., and Schell, J. (1992). Regulation of plant genes specifically induced in developing and mature nitrogen-fixing nodules: *cis*-Acting elements and *trans*-acting factors. In Control of Plant Gene Expression, D.P.S. Verma, ed (Boca Raton, FL: CRC Press), pp. 241–258.

de Bruijn, F.J., Szabados, L., and Schell, J. (1990). Chimeric genes and transgenic plants are used to study the regulation of genes involved in symbiotic plant–microbe interactions. Dev. Genet. **11,** 182–196.

de Bruijn, F.J., Chen, R.C., Fujimoto, S.Y., Pinaev, A., Silver, D., and Szczyglowski, K. (1994). Regulation of nodulin gene expression. Plant Soil **161,** 59–68.

Dehio, C., and de Bruijn, F.J. (1992). The early nodulin gene *SrEnod2* from *Sesbania rostrata* is inducible by cytokinin. Plant J. **2,** 117–128.

Depicker, A., Stachel, S., Dhaese, P., Zambryski, P., and Goodman, H.M. (1982). Nopaline synthase: Transcript mapping and DNA sequence. J. Mol. Appl. Genet. **1,** 561–573.

Dickstein, R.T., Bisseling, T., Reinhold, V.N., and Ausubel, F.M. (1988). Expression of nodule-specific genes in alfalfa root nodules blocked at an early stage of development. Genes Dev. **2,** 677–678.

Dietrich, R.A., Radke, S.E., and Harada, J.J. (1992). Downstream DNA sequences are required to activate a gene expressed in the root cortex of embryos and seedlings. Plant Cell **4,** 1371–1382.

Dreyfus, B.L., and Dommergues, Y.R. (1981). Nitrogen-fixing nodules induced by *Rhizobium* on the stem of the tropical legume *Sesbania rostrata.* FEMS Microbiol. Lett. **10,** 313–317.

Ebert, P., Ha, S.B., and An, G. (1987). Identification of an essential upstream element in the nopaline synthase promoter by stable and transient assays. Proc. Natl. Acad. Sci. USA **84,** 5745–5749.

Finan, T.M., Hirsch, A.M., Leigh, J.A., Johansen, E., Kuldau, G.A., Deegan, S., Walker, G.C., and Signer, E.R. (1985). Symbiotic mutants of *Rhizobium meliloti* that uncouple plant from bacterial differentiation. Cell **40,** 869–877.

Fisher, R.F., and Long, S.R. (1992). *Rhizobium*–plant signal exchange. Nature **357,** 655–660.

Franck, A., Guilley, H., Jonard, G., Richards, K., and Hirth, L. (1980). Nucleotide sequence of cauliflower mosaic virus DNA. Cell **21,** 285–294.

Franssen, H.J., Nap, J.-P., Gloudemans, T., Stiekema, W., Van Dam, H., Govers, F., Louwerse, J., Van Kammen, A., and Bisseling, T. (1987). Characterization of cDNA for nodulin-75 of soybean: A gene product involved in early stages of root nodule development. Proc. Natl. Acad. Sci. USA **84,** 4495–4499.

Fu, H., Kim, S.Y., and Park, W.D. (1995a). High-level tuber expression and sucrose inducibility of a potato *Sus4* sucrose synthase gene require 5′ and 3′ flanking sequences and the leader intron. Plant Cell **7,** 1387–1394.

Fu, H., Kim, S.Y., and Park, W.D. (1995b). A potato *Sus3* sucrose synthase gene contains a context-dependent 3′ element and a leader intron with both positive and negative tissue-specific effects. Plant Cell **7,** 1395–1403.

Gloudemans, T., and Bisseling, T. (1989). Plant gene expression in early stages of *Rhizobium*–legume symbiosis. Plant Sci. **65,** 1–4.

Govers, F., Franssen, H.J., Pieterse, C., Wilmer, J., and Bisseling, T. (1990). Function and regulation of the early nodulin gene *ENOD2.* In Genetic Engineering of Crop Plants, G.W. Lycett and D.W. Grierson, eds (London: Butterworths), pp. 259–269.

Hall, T.C., Ma, Y., Buchbinder, B.U., Pyne, J.W., Sun, S.M., and Bliss, F.A. (1978). Messenger RNA for G1 protein of French bean seeds: Cell-free translation and product characterization. Proc. Natl. Acad. Sci. USA **75,** 3196–3200.

Hirsch, A.M. (1992). Developmental biology of legume nodulation. New Phytol. **122,** 211–237.

Hirsch, A.M., Bhuvaneswari, T.V., Torrey, J.G., and Bisseling, T. (1989). Early nodulin genes are induced in alfalfa root outgrowths elicited by auxin transport inhibitors. Proc. Natl. Acad. Sci. USA **86,** 1244–1248.

Hirsch, A.M., Assad, S., Fang, Y., Wycoff, K., and Loebler, M. (1993). Molecular interactions during nodule development. In New Horizons in Nitrogen Fixation, R. Palacios, J. Moira, and W.E. Newton, eds (Dordrecht, The Netherlands: Kluwer Academic Publishers), pp. 291–296.

Ingelbrecht, I.L.W., Herman, L.M.F., Dekeyser, R.A., Van Montagu, M.C., and Depicker, A.G. (1989). Different 3′ end regions strongly influence the level of gene expression in plant cells. Plant Cell **1,** 671–680.

Jefferson, R.A. (1987). Assaying chimeric genes in plants: The GUS gene fusion system. Plant Mol. Biol. Rep. **5,** 387–405.

Jefferson, R.A., Kavanagh, T.A., and Bevan, M.W. (1987). GUS fusions: β-Glucuronidase as sensitive and versatile gene fusion marker in higher plants. EMBO J. **6,** 3901–3907.

Kijne, J.W. (1992). The *Rhizobium* infection process. In Biological Nitrogen Fixation, G. Stacey, R.H. Burris, and H.J. Evans, eds (New York: Chapman and Hall), pp. 349–398.

Kunkel, T.A. (1985). Rapid and efficient site-specific mutagenesis without phenotypic selection. Proc. Natl. Acad. Sci. USA **82,** 488–498.

Larkin, J.C., Oppenheimer, D.G., Pollock, S., and Marks, M.D. (1993). Arabidopsis *GLABROUS1* gene requires downstream sequences for function. Plant Cell **5,** 1739–1748.

Lauridsen, P., Franssen, H., Stougaard, J., Bisseling, T., and Marker, K.A. (1993). Conserved regulation of the soybean early

nodulin *ENOD2* gene promoter in determinate and indeterminate transgenic root nodules. Plant J. **3,** 483–492.

Lerouge, P., Roche, P., Faucher, C., Maillet, F., Truchet, G., Promé, J.C., and Dénarié, J. (1990). Symbiotic host-specificity of *Rhizobium meliloti* is determined by a sulfated and acylated glucosamine oligosaccharide signal. Nature **344,** 781–784.

Libbenga, K.R., Van Iren, F., Bogers, R.J., and Schraag-Lamers, M.F. (1973). The role of hormones and gradients in the initiation of cortex proliferation and nodule formation in *Pisum sativum* L. Planta **114,** 29–39.

Long, S.R. (1989). *Rhizobium*–legume nodulation: Life together in the underground. Cell **56,** 203–214.

Maniatis, T., Fritsch, E.F., and Sambrook, J. (1989). Molecular Cloning: A Laboratory Manual, 2nd ed. (Cold Spring Harbor, NY: Cold Spring Harbor Laboratory Press).

Mylona, P., Pawlowski, K., and Bisseling, T. (1995). Symbiotic nitrogen fixation. Plant Cell **7,** 869–885.

Nap, J.-P., and Bisseling, T. (1990). Developmental biology of a plant–prokaryote symbiosis: The legume root nodule. Science **250,** 948–954.

Ndoye, I., de Billy, F., Vasse, J., Dreyfus, B., and Truchet, G. (1994). Root nodulation of *Sesbania rostrata.* J. Bacteriol. **176,** 1060–1068.

Odell, J.T., Nagy, F., and Chua, N.-H. (1985). Identification of DNA sequences required for activity of the cauliflower mosaic virus 35S promoter. Nature **313,** 810–812.

Owen, D., and Kuhn, L.C. (1987). Noncoding 3′ sequences of the transferrin receptor gene are required for mRNA regulation by iron. EMBO J. **6,** 1287–1293.

Pankhurst, C.E., Broughton, W.J., and Wieneke, U. (1983). Transfer of an indigenous plasmid of *Rhizobium loti* to other rhizobia and *Agrobacterium tumefaciens.* J. Gen. Microbiol. **129,** 2535–2543.

Pawlowski, K., Klosse, U., and de Bruijn, F.J. (1991). Characterization of a novel *Azorhizobium caulinodans* ORS571 two-component regulatory system, NtrY/NtrX, involved in nitrogen fixation and metabolism. Mol. Gen. Genet. **231,** 124–138.

Pietrzak, M., Shillito, R.D., Hohn, T., and Potrykus, I. (1986). Expression in plants of two bacterial antibiotic resistance genes after protoplast transformation with a new plant expression vector. Nucleic Acids Res. **14,** 5857–5868.

Pingret, J.-L., Journet, E.-P., and Barker, D.G. (1998). *Rhizobium* Nod factor signaling: Evidence for a G protein–mediated transduction mechanism. Plant Cell **10,** 659–672.

Ramlov, K.B., Laursen, N.B., Stougaard, J., and Marcker, K.A. (1993). Site-directed mutagenesis of the organ-specific element in the soybean leghemoglobin *lbc3* gene promoter. Plant J. **4,** 577–580.

Sanders, P.R., Winter, J.A., Barnason, A.R., Rogers, S.G., and Fraley, R.T. (1987). Comparison of cauliflower mosaic virus 35S and nopaline synthase promoters in transgenic plants. Nucleic Acids Res. **15,** 1543–1558.

Silver, D.L. (1996). The *Sesbania rostrata* Early Nodulin Gene *SrEnod2* as a Marker for Cytokinin Signal Transduction. PhD Dissertation (East Lansing, MI: Michigan State University).

Silver, D.L., Pinaev, A., Chen, R., and de Bruijn, F.J. (1996). Posttranscriptional regulation of the *Sesbania rostrata* early nodulin gene *SrEnod2* by cytokinin. Plant Physiol. **112,** 559–567.

Stougaard, J., Sandal, N.N., Gron, A., Kühle, A., and Marcker, K.A. (1987). 5′-Analysis of the soybean leghemoglobin *lbc3* gene: Regulatory elements required for promoter activity and organ specificity. EMBO J. **6,** 3565–3569.

Szabados, L., Ratet, P., Grunenberg, B., and de Bruijn, F.J. (1990). Functional analysis of the *Sesbania rostrata* leghemoglobin *glb*3 gene 5′-upstream region in transgenic *Lotus corniculatus* and *Nicotiana tabacum* plants. Plant Cell **2,** 973–986.

Szczyglowski, K., and Legocki, A.B. (1990). Isolation and nucleotide sequence of a cDNA clone encoding nodule-specific (hydroxy) proline-rich protein *LEnod2* from yellow lupin. Plant Mol. Biol. **15,** 361–363.

Szczyglowski, K., Szabados, L., Fujimoto, S.F., Silver, D., and de Bruijn, F.J. (1994). Site-specific mutagenesis of the nodule-infected cell expression (NICE) element and the AT-rich element ATRE-BS2* of the *Sesbania rostrata* leghemoglobin g*lb*3 promoter. Plant Cell **6,** 317–332.

Taylor, C.B., Bariola P.A., Del Cardayre, S.B., Raines, R.T., and Green, P.J. (1993). RNS2: A senescence-associated RNase of *Arabidopsis* that diverged from the S-RNases before speciation. Proc. Natl. Acad. Sci. USA **90,** 5118–5122.

Tempe, J., and Casse-Delbart, F. (1989). Plant gene vectors and genetic transformation: *Agrobacterium* Ri plasmids. In Cell Culture and Somatic Cell Genetics of Plants, Vol. 6, J. Schell and I.K. Vasil, eds (San Diego, CA: Academic Press), pp. 25–49.

Thimann, K.V. (1936). On the physiology of the formation of nodules on legume roots. Proc. Natl. Acad. Sci. USA **22,** 511–515.

Thornburg, R.W., An, G., Cleveland, T.E., Johnson, R., and Ryan, C.A. (1987). Wound-inducible expression of a potato inhibitor II–chloramphenicol acetyltransferase gene fusion in transgenic tobacco plants. Proc. Natl. Acad. Sci. USA **84,** 744–748.

Tjepkema, J.D., and Yocum, C.S. (1974). Measurement of oxygen partial pressure within soybean nodules by oxygen microelectrodes. Planta **119,** 351–360.

Trainor, C.D., Stamler, S.J., and Engel, J.D. (1987). Erythroid-specific transcription of the chicken histone H5 gene is directed by a 3′ enhancer. Nature **328,** 827–830.

Truchet, G., Roche, P., Lerouge, P., Vasse, J., Camut, S., de Billy, F., Promé, J.C., and Dénarié, J. (1991). Sulphated lipooligosaccharide signals from *Rhizobium meliloti* elicit root nodule organogenesis in alfalfa. Nature **351,** 670–673.

Tsien, H.C., Dreyfus, B.L., and Schmidt, E.L. (1983). Initial stages in the morphogenesis of nitrogen-fixing stem nodules of *Sesbania rostrata.* J. Bacteriol. **156,** 888–897.

Van de Wiel, C., Scheres, B., Franssen, H., Van Lierop, M.J., Van Lammeren, A., Van Kammen, A., and Bisseling, T. (1990a). The early nodulin transcript ENOD2 is located in the nodule parenchyma (inner cortex) of pea and soybean root nodules. EMBO J. **9,** 1–7.

Van de Wiel, C., Norris, J.H., Bochenek, B., Dickstein, R., Bisseling, T., and Hirsch, A.M. (1990b). Nodulin gene expression and ENOD2 localization in effective, nitrogen-fixing and ineffective, bacteria-free nodules of alfalfa. Plant Cell **2,** 1009–1017.

Van Kammen, A. (1984). Suggested nomenclature for plant genes involved in nodulation and symbiosis. Plant Mol. Biol. Rep. **2,** 43–45.

Verma, D.P.S. (1992). Signals in root nodule organogenesis and endocytosis of *Rhizobium*. Plant Cell **4,** 373–382.

Verma, D.P.S., and Delauney, A.J. (1988). Root nodule symbiosis: Nodulins and nodulin genes. In Temporal and Spatial Regulation of Plant Genes, R.B. Goldberg and D.P.S. Verma, eds (New York: Springer-Verlag), pp. 169–199.

Verwoerd, T.C., Dekker, B.M.M., and Hoekema, A. (1989). A small-scale procedure for the rapid isolation of plant RNAs. Nucleic Acids Res. **17,** 2362.

Vijn, I., das Neves, L., Van Kammen, A., Franssen, H., and Bisseling, T. (1993). Nod factors and nodulation in plants. Science **260,** 1764–1765.

Weiss, I.M., and Liebhaber, S.A. (1995). Erythroid cell-specific mRNA stability elements in the α2-globin 3′ nontranslated region. Mol. Cell. Biol. **15,** 2457–2465.

Witty, J.F., Minchin, F.R., Skot, L., and Sheehy, J.E. (1986). Nitrogen fixation and oxygen in legume nodules. Oxford Surv. Plant Mol. Cell Biol. **3,** 275–314.

Yang, W.-C., de Blank, C., Meskiene, I., Hirt, H., Bakker, J., Van Kammen, A., Franssen, H., and Bisseling, T. (1994). *Rhizobium* Nod factors reactivate the cell cycle during infection and nodule primordium formation, but the cycle is only completed in primordium formation. Plant Cell **6,** 1415–1426.